Journal of Cellular Biochemistry 97:782–794 (2006)

Tumor Necrosis Factor-Related Apoptosis-Inducing Ligand (TRAIL) Regulates Endothelial Nitric Oxide Synthase (eNOS) Activity and Its Localization Within the Human Vein Endothelial Cells (HUVEC) in Culture

Roberta Di Pietro,[1] Maria A. Mariggiò,[2,3] Simone Guarnieri,[2,3] Silvia Sancilio,[1] Annalisa Giardinelli,[3] Sara Di Silvestre,[3] Agostino Consoli,[3,4] Giorgio Zauli,[5] and Assunta Pandolfi[1,3]*

[1]Department of Biomorphology, ''G. d'Annunzio'' University, Chieti-Pescara, Italy
[2]Laboratory of Cellular Physiology, Department of Drug Sciences, ''G. d'Annunzio'' University, Chieti-Pescara, Italy
[3]Aging Research Center, Ce.S.I., ''G. d'Annunzio'' University Foundation, Chieti-Pescara, Italy
[4]Department of Medicine and Aging Sciences, ''G. d'Annunzio'' University, Chieti-Pescara, Italy
[5]Department of Normal Human Morphology, University of Trieste, Trieste, Italy

Abstract We have recently demonstrated that tumor necrosis factor-related apoptosis-inducing ligand (TRAIL) increases endothelial nitric oxide synthase (eNOS) phosphorylation, NOS activity, and nitric oxide (NO) synthesis in cultured human umbilical vein endothelial cells (HUVEC), without inducing apoptotic cell death. Although an important factor that regulates eNOS activity is its localization within the cells, little is known about the role of TRAIL in the regulation of eNOS trafficking among cellular compartments and the cytoskeleton involvement in this machinery. Then, we did both quantitative and semi-quantitative evaluations with biochemical assays and immune fluorescence microscopy in the presence of specific inhibitors of NOS activity as well as of cytoskeletal microtubule structures. In our cellular model, TRAIL treatment not only increased NO levels but also caused a time-dependent NO migration of fluorescent spots from the plasma membrane to the inner part of the cells. In unstimulated cells, most of the eNOS was localized at the cell membranes. However, within 10 min following addition of TRAIL, nearly all the cells showed an increased cytoplasm localization of eNOS which appeared co-localized with the Golgi apparatus at a higher extent than in unstimulated cells. These effects were associated to an increased formation of trans-cytoplasm stress fibers with no significant changes of the microtubule network. Conversely, microtubule disruption and Golgi scattering induced with Nocodazole treatment inhibited TRAIL-increased NOS activity, indicating that, on cultured HUVEC, TRAIL ability to affect NO production by regulating eNOS sub-cellular distribution is mediated by cytoskeleton and Golgi complex modifications. J. Cell. Biochem. 97: 782–794, 2006.

Key words: TRAIL; eNOS intracellular localization; endothelial cells

Tumor necrosis factor-related apoptosis-inducing ligand (TRAIL) is a member of the structurally related TNF family of cytokines which influence a variety of functions among which are cell death, immune response, and inflammation [Wiley et al., 1995; Baker and Reddy, 1996]. Although only a few years ago TRAIL was known for being able to induce apoptosis in a number of tumor cell lines [Ashkenazi and Dixit, 1999; Secchiero et al., 2001], new additional non-apoptotic effects have been recently described both in normal primary cells and, unexpectedly, in neoplastic cell lines [Ehrhardt et al., 2003; Secchiero et al., 2003, 2004; Di Pietro and Zauli, 2004]. TRAIL

Roberta Di Pietro and Maria A. Mariggiò contributed equally to this study.

Grant sponsor: MIUR (Italian Ministry of University and Research); Grant sponsor: COFIN 2004 (to AP); Grant number: 2004050541_002; Grant sponsor: COFIN 2004 (to RDP); Grant number: 2004065810_004; Grant sponsor: University of Chieti (ex MURST 60%) (to AP and RDP).

*Correspondence to: Assunta Pandolfi, PhD, "G. d'Annunzio" University Chieti-Pescara, Aging Research Center, Ce.S.I., "G. d'Annunzio" University Foundation, Room 458, Via Colle dell'Ara, 66013 Chieti, Italy.
E-mail: pandolfi@unich.it

Received 6 June 2005; Accepted 6 September 2005
DOI 10.1002/jcb.20686

acts following interaction with four high affinity membrane receptors: TRAIL-R1 (DR4) and TRAIL-R2 (DR5) transduce apoptotic signals and are commonly known as death receptors [Pan et al., 1997; Walczak et al., 1997]; TRAIL-R3 (DcR1) and TRAIL-R4 (DcR2) do not contain death domains and are unable to transduce death signals [Pan et al., 1997; Degli Esposti et al., 1997a,b]. It has been proposed that TRAIL-R3 and TRAIL-R4 function as decoy receptors protecting normal cells, including endothelial cells, from apoptosis [Zhang et al., 2000; Secchiero et al., 2003].

In a recent study [Zauli et al., 2003] we demonstrated that, on endothelial cells, TRAIL is able to modulate the production of nitric oxide (NO), a biologically active gas which is generated from the precursor arginine by a family of enzymes termed NO synthases (NOS), cloned and identified in various organs as three different isoforms NOS I, II, and III [Ortiz and Garvin, 2003]. NOS III, originally isolated from vascular endothelial cells, was termed endothelial nitric oxide synthase (eNOS). NO produced by eNOS plays an important physiological role in the regulation of a variety of cardiovascular functions such as vascular tone and endothelial cell survival and migration [Hobbs et al., 1999]. eNOS was originally characterized as a calcium/calmodulin-dependent enzyme [Busse and Mulsch, 1990] and, although this is the primary means by which eNOS activity is controlled, additional post-transcriptional mechanisms of enzyme activity regulation have been discovered [Ortiz and Garvin, 2003]. Among these, the Akt-dependent serine phosphorylation of eNOS has been observed in endothelial cells in response to a variety of stimuli, including TRAIL [Ortiz and Garvin, 2003; Zauli et al., 2003]. In addition, recently it has been reported that a proper membrane localization, very likely both at the Golgi complex and at the plasma membrane level [Fulton et al., 2002, 2004], is necessary for optimal functioning and receptor-mediated stimulation of eNOS activity [Michel and Feron, 1997; Michel, 1999]. On the other hand, other authors have reported that eNOS translocates to a detergent-insoluble cell fraction after stimulation both with calcium-mobilizing agents, such as bradykinin, and with calcium-independent stimuli, such as shear stress [Govers et al., 2002].

Currently, very little is known about the TRAIL-regulated activation and movement of eNOS among different sub-cellular compartments or the protein machinery involved in this cellular function. Therefore, using human umbilical vein endothelial cells (HUVEC) as a model system, we have investigated whether TRAIL, known to enhance eNOS phosphorylation, NOS activity, and NO synthesis [Zauli et al., 2003], was also able to affect eNOS trafficking among different sub-cellular compartments. To assess whether cytoskeleton components were possibly involved in this machinery, microtubule depolymerizing agents were employed.

MATERIALS AND METHODS

Reagents

M199 was from BioWhittaker (Walkersville, MD). EBM was from Clonetics-BioWhittaker (Walkersville, MD). Fetal calf serum (FCS) and Dulbecco's phosphate buffered saline (PBS) were from Mascia Brunelli (Milan, Italy). Heparin was from Pfizer Italia (Latina, Italy). L-arginine hydrochloride, horse serum from platelet poor plasma, collagenase, endothelial cell growth factor (ECGF), bovine serum albumin (BSA), $CaCl_2$, BH_4 (tetrahydrobiopterin), the microtubule depolymerizing agent Nocodazole and Ionomycin were purchased from Sigma-Aldrich (Milan, Italy). Both recombinant Histidine6-tagged TRAIL and Histidine6 control peptide were produced in bacteria, purified by chromatography on Ni^{++} affinity resin, and tested for cytotoxic activity on the TRAIL-sensitive Jurkat cell line, as previously described [Secchiero et al., 2001]. The NO synthase (NOS) inhibitor *N*-nitro-L-arginine methyl ester (L-NAME) and the NO-reactive dye 4,5-diaminofluorescein diacetate (DAF-2DA) were from Calbiochem (La Jolla, CA). DAN Assay was from Cayman Chemical Company (Ann Arbor, MI). L-[^{3}H]-arginine monohydrochloride was from Perkin Elmer (Boston, MA). Dowex AGWX8-200 Resin was from Aldrich, Steinheim, Germany. The ECNOS/NOS type III antibody was purchased from Transduction Laboratories (Lexington, KY). The primary antibody to the Golgi complex was kindly provided by Dr. Antonella De Matteis (Mario Negri Sud Institute, S. Maria Imbaro, Italy). The proliferating cell nuclear antigen (PCNA) rabbit polyclonal IgG antibody was from Santa Cruz (Santa Cruz, CA). Anti α-tubulin mouse primary antibody, Phalloidin Alexa-594, Alexa-568 goat anti-mouse, Alexa-488 goat anti-rabbit, and Alexa-

488 goat anti-mouse secondary antibodies were from Molecular Probes (Eugene, OR).

Cell Cultures

Primary HUVEC were obtained from umbilical cords of randomly selected healthy mothers delivering at the University Hospital in Chieti. After perfusion of umbilical cords with 0.1% collagenase at 37°C, HUVEC were grown on 0.2% gelatin-coated tissue culture plates in M199 endothelial growth medium supplemented with 20% FCS, 10 μg/ml heparin, and 50 μg/ml ECGF.

For all experiments, cells were used between the 3rd and 5th passage in vitro (sub-confluence) and serum-starved for 2 h in EBM (phenol red-free endothelial basal media) supplemented with 1% platelet-deprived horse serum and 100 μM L-arginine.

Measurement of Extracellular NO Production With DAN Assay

For measurement of NO production, after serum starvation HUVEC were incubated for 10 min with appropriate stimuli. The media were then collected, spun 1 min at 2,000*g*, transferred to a new tube, and subjected to the NO production assay. The DAN assay was performed according to the method of Misko et al. [1993] with minor modifications. In brief, DAN was dissolved in 0.62 N HCl at a concentration of 0.05 mg/ml. Aliquots of HUVEC media (10 μl) were placed into 96-well plates in triplicate. Media were void of any interfering components such as dithiothreitol, protein, FCS, phenol red, or hemoglobin. DAN (10 μl) was added to each well for 10 min at room temperature. Then, 20 μl of 2.8N NaOH were added to each well, and the plate was read on a Canberra Packard Fluoro Count (Milan, Italy) (excitation 360 nm, emission 440 nm). Standard curves were daily made with sodium nitrite ranging from 0 to 600 pmoles in phenol red-free EBM. In selected experiments, NO^{3-} in culture medium was reduced to NO^{2-} with nitrate reductase (14 mU) and NADPH (40 μM) at room temperature for 5 min, media were then collected and subjected to the DAN assay as described above.

Localization of Intracellular NO Production With DAF-2-DA

For confocal measurement of intracellular NO production, HUVEC were loaded with the NO-reactive dye DAF-2DA at the final concentration of 10 μM for 30 min at 37°C. Cells were then washed three times in EBM and transferred into an Attofluor chamber (Molecular Probes), before TRAIL (1 μg/ml) administration. During the experiments, the cells were kept at room temperature in the dark and each coverslip was examined within a period of time that did not exceed 30 min. Fluorescence images were obtained using a Bio-Rad MRC-1024 ES confocal system (Bio-Rad Microscience Ltd., Hemel Hempstead, UK) equipped with a ZEISS Axiovert 100 inverted microscope with a 63 × 1.25 NA PLAN NEOFLUAR oil immersion objective lens (ZEISS, Jena, Germany). The Kr/Ar laser potency, photo-multiplier, and pinhole size were kept constant for the entire experimental procedure. Images were acquired using the Laser Sharp 3.1 software (Bio-Rad). The DAF-2DA green fluorescence was recorded using a 488 nm laser excitation line and a 522 nm band pass emission filter (bandwidth ±32 nm). Images were sampled every 2 s, stored, and analyzed. The acquired images were processed in pseudocolor according to a reference color scale ranging from blue to red corresponding to low (blue) and high (red) intracellular NO levels, respectively. In some experiments, L-NAME was added 45 min before loading with DAF-2DA and NO production was visualized as reported. Traces deriving from total cellular area were calculated as F/F0, where F is the fluorescence emission of a single DAF-2DA loaded cell at time intervals ranging from 2 to x s and F0 is the fluorescence emission of the same cell at time 0.

Assay of Nitric Oxide Synthase (NOS) Activity

HUVEC grown to sub-confluence in 6-well plates, after serum starvation, were treated with TRAIL (1 μg/ml) and/or Nocodazole (10 μM, with 45 min pre-incubation) for 10 min at room temperature. After treatment, cells were detached with trypsin/EDTA (0.05/0.02% v/v), washed with PBS, then resuspended in 1 ml of reaction buffer (20 mM HEPES, 0.5 mM EDTA, 1 mM dithiothreitol, pH 7.2), and sonicated on ice with three bursts of 10 s. In each test tube, the following reagents were added to 100 μl lysate at the final concentrations: 2 mM NADPH, 1.5 mM $CaCl_2$, 0.1 mM BH_4, 2.5 μCi L-[^{3}H]-arginine (0.4 μM) [Pandolfi et al., 2003]. After a 15 min incubation at 37°C, the reaction was stopped by adding 2 ml HEPES–Na pH 6

containing 2 mM EDTA; the entire reaction mixture was applied to 2-ml columns of Dowex AG50WX-8 (Na^+ form) and eluted with 4 ml of water. The radioactivity corresponding to the [^{3}H]-citrulline content in the eluate was measured with a liquid scintillation analyzer (Packard Bio Science company, Meriden, CT). NOS activity was expressed as pmoles citrulline/min/mg cell protein. In some experiments, L-NAME (1 mM) was added 45 min before TRAIL stimulation.

Cells Preparations for Immunofluorescence Staining

In these sets of experiments, HUVEC cultures were treated with TRAIL (1 μg/ml) for 10 min with or without a 45 min pre-incubation with L-NAME (1 mM) or, in some experiments (eNOS/Golgi immune labeling and actin/tubulin staining) with Nocodazole (10 μM, with 45 min pre-incubation). At the end of treatment, cells were fixed for 10 min with a 3% paraformaldehyde solution at room temperature Dulbecco's phosphate buffered saline 1× pH 7.6 supplemented with 2% saccharose. Then, cell membranes were permeabilized for 5 min at room temperature with a pH 7.6 solution containing 0.5% Triton X-100/20 mM HEPES, 300 μM saccharose, 50 mM NaCl, 3 mM $MgCl_2$.

eNOS/nucleus immune labeling. After membrane permeabilization, cells were incubated with 10% BSA in 1× Dulbecco's phosphate-buffered saline for 30 min at room temperature, followed by a 45 min incubation at room temperature with ECNOS/NOS type III antibody at the final concentration of 5 μg/ml (in 1% BSA/PBS), and PCNA antibody (1:1,000 in 1% BSA/PBS). Alexa-568 goat anti-mouse (1:100 in 1% BSA/PBS) and Alexa-488 goat anti-rabbit (1:100 in 1% BSA/PBS) secondary antibodies were left in incubation for 1 h at room temperature.

eNOS/Golgi immune labeling. After membrane permeabilization, cells were treated as described above, using primary antibodies against eNOS and Golgi complex (1:1,000 in 1% BSA/PBS).

Actin/tubulin staining. After membrane permeabilization, cells were incubated with 10% BSA in 1× Dulbecco's phosphate-buffered saline for 45 min at room temperature, followed by a 60 min incubation at 37°C with anti α-tubulin (1:100 in 1% BSA/PBS) monoclonal antibody. Goat anti-mouse Alexa 488 (1:100 in 1% BSA/PBS) secondary antibody was left in incubation for 1 h at 37°C. Finally, cells were labeled with Phalloidin Alexa-594 (1:50) for 30 min at 37°C. All the slides were mounted with Slowfade (Molecular Probes), and observed with a ZEISS 510 META confocal microscope. Images were acquired using LSM 510 META confocal microscopy software (rel. 3.0, ZEISS).

eNOS/Golgi Colocalization Analysis

Colocalization analysis on images was performed using ImageJ Software (Rasband, W.S., ImageJ, National Institutes of Health, Bethesda, Maryland, http://rsb.info.nih.gov/ij/, 1997–2004) and the image correlator plus plugin. The calculations were based on Pearson's correlation coefficient which is one of the standard procedures to describe the degree of overlapping between two patterns [Zanella et al., 2002]. In order to estimate the contribution of one color channel in the co-localized areas of the image, an additional set of co-localization coefficients, C_{green} and C_{red}, were calculated according to the following equations:

$$C_{green} = \frac{\sum_i G_{i,color}}{\sum_i G_i} \quad \text{and} \quad C_{red} = \frac{\sum_i R_{i,color}}{\sum_i R_i}$$

The two coefficients C_{red} and C_{green} are proportional to the amount of fluorescence of the colocalizing object in each voxel, relating to the total amount of fluorescence in that voxel; their values are between 0 and 1 and a value of 0 indicates that there is no colocalization, while a value of 1 indicates that there is complete colocalization.

Statistical Analysis

All quantitative data are reported as mean ± SD. Statistical analyses were performed using the one-way ANOVA or Student t-test. Values of $P < 0.05$ were considered statistically different.

RESULTS

TRAIL Stimulates NO Synthesis in HUVEC

We have previously shown that cultured HUVEC express high affinity TRAIL receptors and respond to TRAIL treatment with an increase in NO intracellular production [Zauli et al., 2003]. Here, to evaluate the possible extracellular NO release induced by TRAIL, we measured NO levels in the culture medium of HUVEC through the DAN assay. As shown in

Figure 1, after 10 min of incubation, a significant increase in NO extracellular products was found in conditioned media of TRAIL-stimulated cells, as compared to control cells. As expected, in our cellular model ionomycin (positive control) significantly increased NO production. Pre-incubation with L-NAME, a competitive inhibitor of NOS, induced a significant decrease in NO levels both in ionomycin- and TRAIL-treated samples, confirming the NOS-dependency of this phenomenon (Fig. 1).

In parallel, to follow real time NO intracellular production, we loaded cells with DAF-2DA before appropriate stimuli. Fluorescent spots of different size indicated the basal NO production in HUVEC, as shown in Figure 2 (control panels 2A,B). It was interesting to note, upon TRAIL administration, an evident and time-dependent migration of the spots towards the peri-nuclear area in at least the 35% of the cells (Fig. 2A), which was completely abrogated by pre-treatment of the cells with L-NAME (Fig. 2B). It is worth noting that the TRAIL-stimulated peak of NO release (F/F0 = 1.4), observed after 327 s, was twofold increased in comparison with TRAIL-induced NO release upon cell pre-treatment with L-NAME (F/F0 = 0.7), a competitive inhibitor of NOS. In parallel experiments, to better quantify NOS activity, conversion of ^{3}H-Arginine into L-[^{3}H]-Citrulline was assessed in HUVEC lysates (Fig. 6). As expected on the basis of the DAN and DAF-2DA data illustrated above, TRAIL treatment induced a significant ($P < 0.001$) increase in NOS activity, which was completely abrogated by pre-treatment of the cells with L-NAME (Fig. 6).

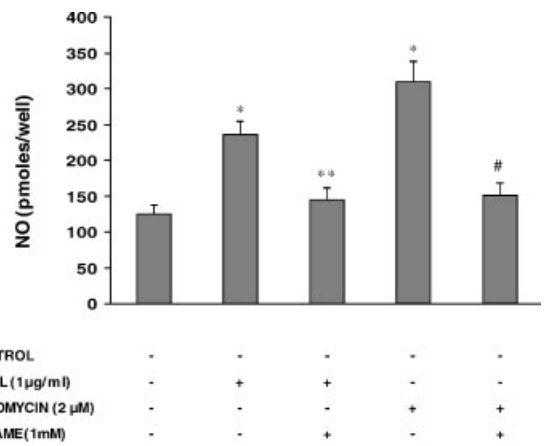

Fig. 1. Tumor necrosis factor-related apoptosis-inducing ligand (TRAIL)-increased extracellular nitric oxide (NO) levels. Extracellular NO levels were quantified in the culture medium of human umbilical vein endothelial cells (HUVEC) exposed for 10 min to different stimuli. Data, expressed as pmol/well, are the mean values ± SD of three independent experiments ($^{*}P < 0.001$ vs. control, $^{**}P < 0.005$ vs. TRAIL and $^{\#}P < 0.001$ vs. Ionomycin).

eNOS Intracellular Localization Is Modified by TRAIL Treatment

To better assess whether TRAIL-stimulated NO increased levels in HUVEC were associated to eNOS redistribution, cells were treated for 10 min with 1 μg/ml TRAIL, in the presence or absence of L-NAME, and labeled with fluorescent markers to follow intracellular localization of eNOS. As shown in Figure 3, immune staining of control HUVEC using eNOS monoclonal antibody revealed a clear pattern of immune fluorescence; instead, no staining was observed when non-immune mouse IgG_1 was used as the primary antibody in identically processed samples (not shown). Quantitative analyses of the membrane-associated eNOS in control endothelial cells showed that in about 70% of the cells, total immune reactivity was usually not uniform: there were often large patches of eNOS-positive membranes located around the nucleus (stained with anti-PCNA antibody) and immediately adjacent to eNOS-negative areas (Fig. 3, control). Importantly, when HUVEC were treated with TRAIL (1 μg/ml, 10 min), the pattern of eNOS immune staining markedly changed as compared with untreated cells (Fig. 3, TRAIL). In fact, TRAIL-treated samples displayed a significant cytoplasm redistribution of eNOS with a stronger immune staining in the distinct ring pattern around the nucleus, as well as at the plasma membrane. The L-NAME pre-incubation completely blocked TRAIL-induced eNOS redistribution (Fig. 3, TRAIL + L-NAME), while L-NAME used alone did not significantly affect eNOS localization (Fig. 3, L-NAME).

To better characterize eNOS intracellular localization, HUVEC were double stained with anti-eNOS and anti-Golgi complex antibodies. The confocal microscopy analysis performed with ImageJ Software, showed that HUVEC cells displayed a diffuse fluorescent red signal (Fig. 4, control) colocalized at the Golgi complex with C_{red} 1.00 and C_{green} 0.751. The administration of 1 μg/ml TRAIL (Fig. 4, TRAIL) determined an increase in C_{green} from 0.751 to 1.0, whereas, as compared to control, the pretreatment with 1 mM L-NAME before TRAIL stimulation did not significantly modify

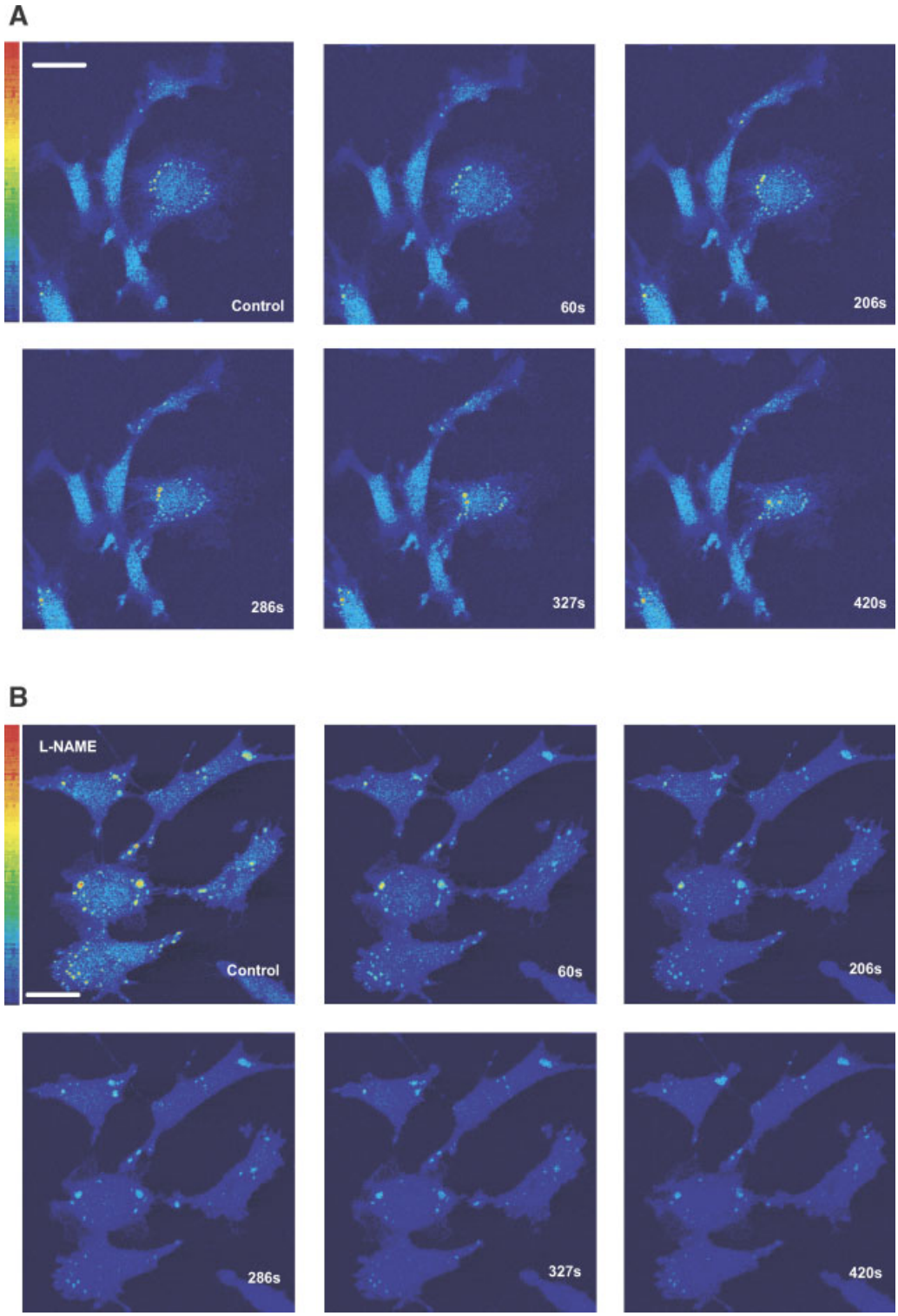

Fig. 2. TRAIL-induced intracellular NO production. HUVEC loaded with DAF-2DA, a fluorescent indicator of NO production, before exposure to TRAIL (1 μg/ml) in the absence (**panel A**) and presence (**panel B**) of L-NAME (1 mM). Images were acquired before (control, recording eNOS basal activity) and after TRAIL stimulation (60, 206, 286, 327, and 420 s). The pseudo-color bar located on the left side of the confocal images indicates a reference color scale ranging from blue to red related to low (blue) and high (red) intracellular NO levels, respectively. Bar = 20 μm. [Color figure can be viewed in the online issue, which is available at www.interscience.wiley.com.]

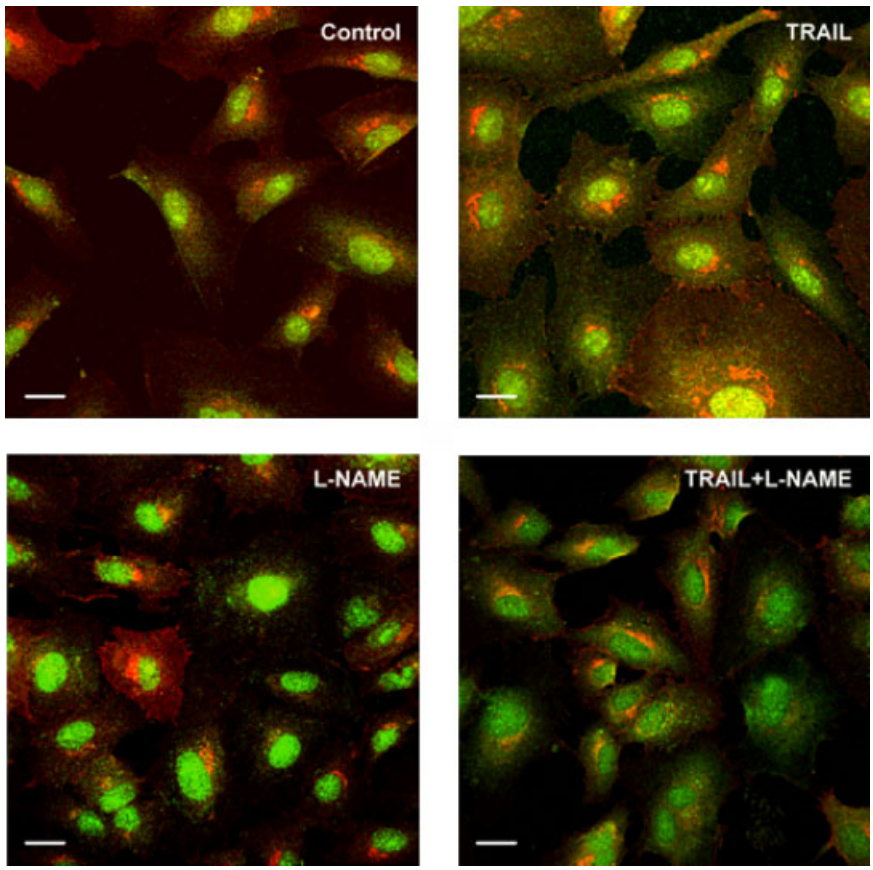

Fig. 3. TRAIL-modulated eNOS intracellular localization. HUVEC treated for 10 min with TRAIL (1 μg/ml) in the presence or absence of L-NAME (1 mM) and L-NAME (1 mM) alone. Cells were immune labeled with anti-eNOS (red fluorescence) and anti-PCNA (green fluorescence) monoclonal antibodies directed against eNOS and nuclei, respectively. Bar = 20 μm. [Color figure can be viewed in the online issue, which is available at www.interscience.wiley.com.]

the colocalization coefficient (C_{green} 0.783; Fig. 4, TRAIL + L-NAME). No significant differences were found after L-NAME treatment alone, as compared to control (C_{green} 0.877; Fig. 4, L-NAME).

In order to verify the importance of a well-preserved Golgi apparatus for TRAIL-stimulated eNOS activity, cells were pre-incubated for 45 min with 10 μM Nocodazole and then, in presence or absence of TRAIL, stimulated for 10 min with this known microtubule depolymerizing agent, which plays also a central role in the juxta-nuclear localization of the Golgi complex [Yang and Storrie, 1998]. As expected, Nocodazole treatment induced Golgi complex scattering and it was interesting to note that, in presence or absence of TRAIL, eNOS showed a spot-like location, mainly at the peri-nuclear area, resembling vesicles of the trans-Golgi network. As compared to C_{green} values (1.00) after TRAIL treatment, the extent of eNOS/Golgi complex colocalization was not significantly changed upon Nocodazole treatment (C_{green} 0.923 and 0.908, Fig. 4; Nocodazole and TRAIL + Nocodazole, respectively). This suggests that the localization of the enzyme at the "intact" Golgi complex may be important for TRAIL-induced eNOS activity as demonstrated by the reduction (almost to 50%) in eNOS activity after Nocodazole treatment (Fig. 6). This indicates that within these scattered Golgi compartments eNOS might be kept inactive and, especially, the enzyme trafficking might be inhibited, as shown by low levels of eNOS cytoplasm localization (Fig. 4, panels Nocodazole and TRAIL + Nocodazole).

TRAIL Induces Cytoskeleton Modifications Related to NO Production

In order to further investigate the potential role of other sub-cellular components involved in TRAIL-mediated eNOS trafficking, we studied

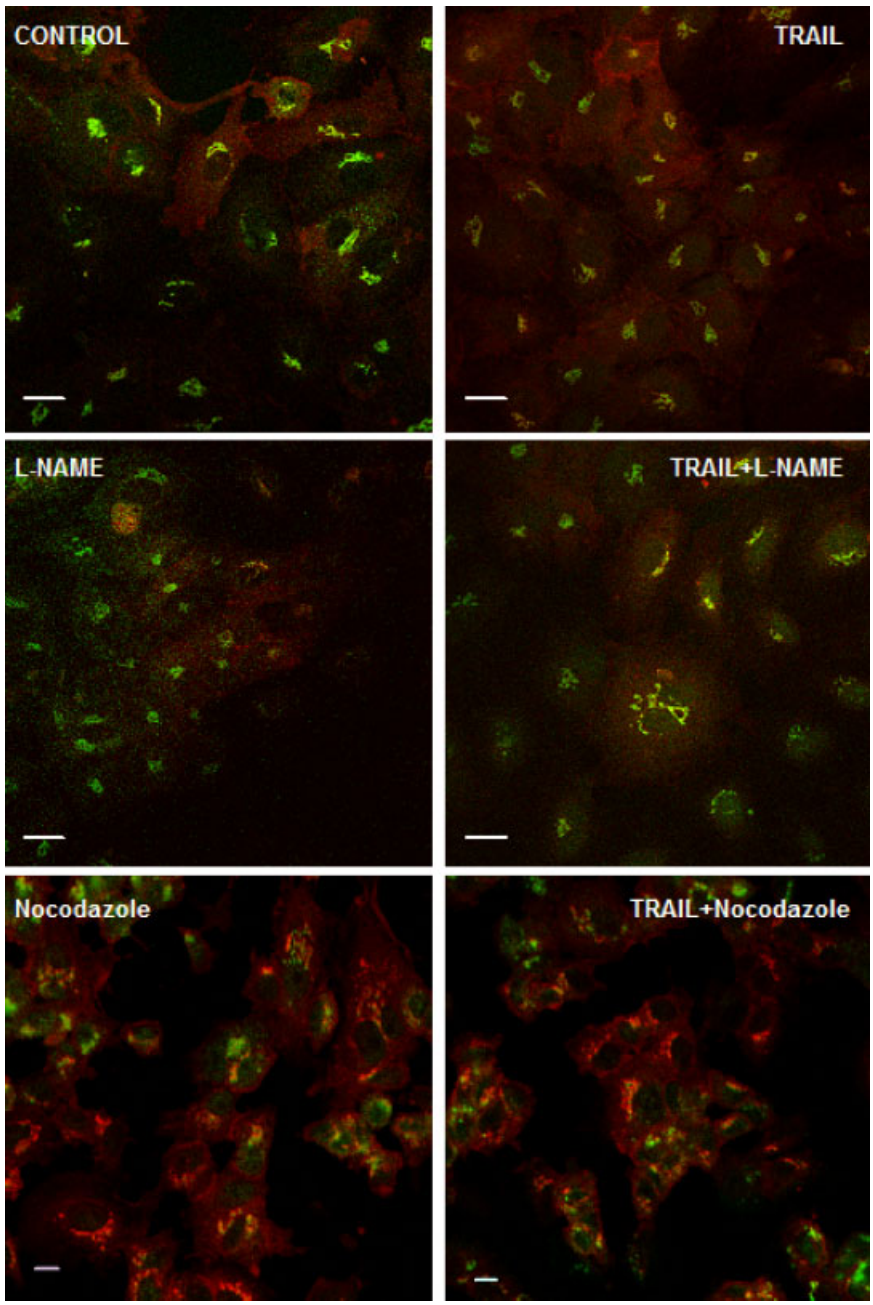

Fig. 4. TRAIL-modulated eNOS and Golgi complex co-localization. HUVEC were treated for 10 min with TRAIL (1 μg/ml) in the presence or absence of L-NAME (1 mM) and L-NAME (1 mM) alone. Cells were immune labeled with anti-eNOS (red fluorescence) and anti-Golgi (green fluorescence) monoclonal antibodies directed against eNOS and Golgi complex, respectively. Bar = 20 μm. [Color figure can be viewed in the online issue, which is available at www.interscience.wiley.com.]

the organization of the actin and tubulin cytoskeleton network, in the presence or absence of 10 μM Nocodazole. First, we analyzed the modifications triggered (within 10 min) by TRAIL treatment on these cytoskeleton components. As shown in Figure 5, TRAIL was able to increase the formation of trans-cytoplasm stress fibers and did not induce microtubule depolymerization. It was interesting to note that both these TRAIL effects were significantly inhibited in the presence of L-NAME (Fig. 5), indicating the NOS-dependency of these phenomena. According to the notion that the state of actin and microtubule polymerization can

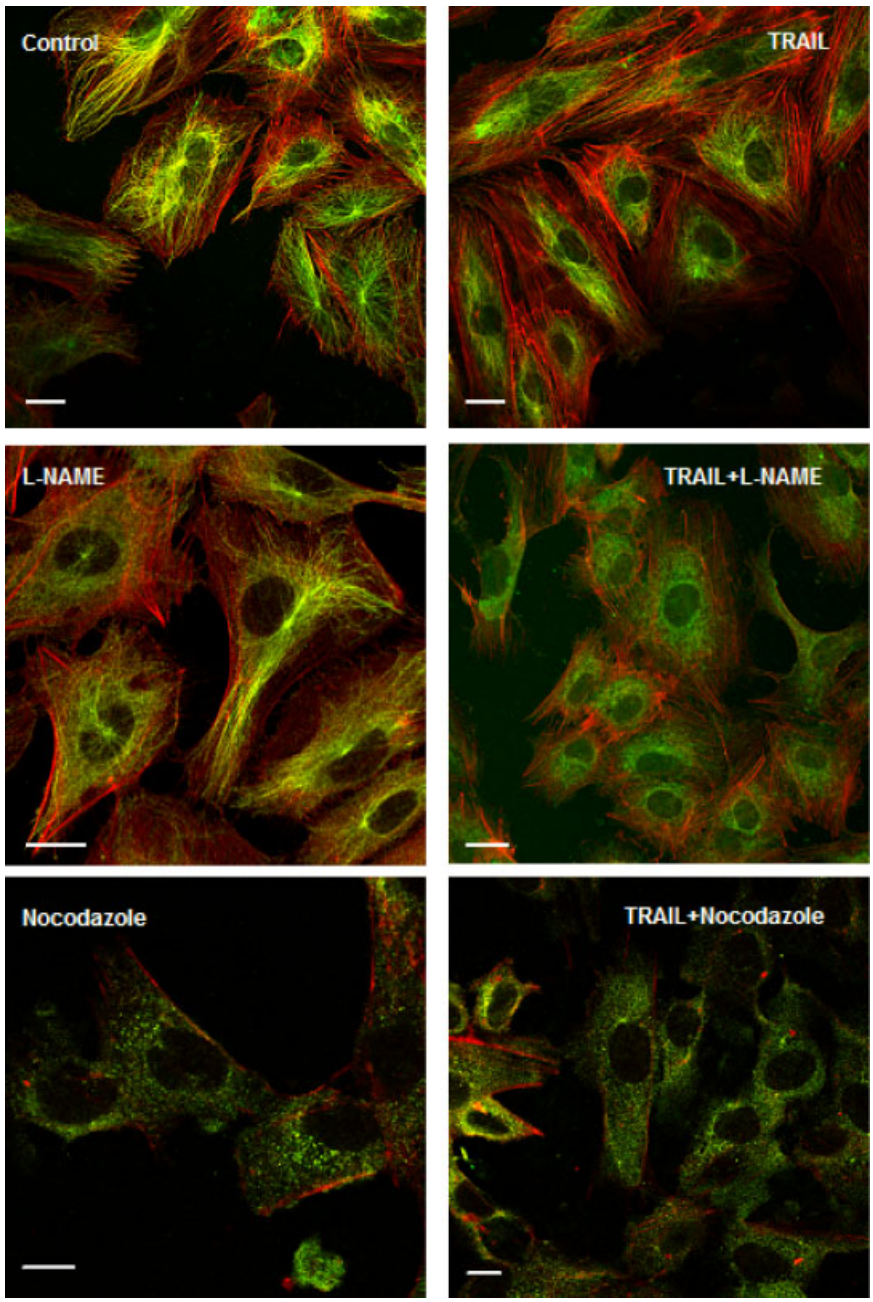

Fig. 5. TRAIL-induced cytoskeleton modifications. HUVEC were treated for 10 min with TRAIL (1 μg/ml) in the presence or absence of L-NAME (1 mM) and L-NAME (1 mM) alone. Cells were stained with phalloidin Alexa 594 (red fluorescence) and anti α-tubulin monoclonal antibody revealed with anti IgG conjugated with Alexa 488 (green fluorescence), labeling the actin and microtubule network, respectively. Bar = 20 μm. [Color figure can be viewed in the online issue, which is available at www.interscience.wiley.com.]

affect endothelial cell eNOS activity and NO production, we demonstrated that TRAIL induced both cytoskeleton reorganization and a concomitant stimulation of NOS activity (Figs. 5 and 6, respectively). These TRAIL effects were significantly inhibited by Nocodazole, which, inducing microtubule depolymerization (Fig. 5, panel Nocodazole and TRAIL + Nocodazole), lead to a significant decrease in NOS activity (Fig. 6), to confirm the notion that the state of cytoskeleton polymerization can affect endothelial cell eNOS activity and NO production.

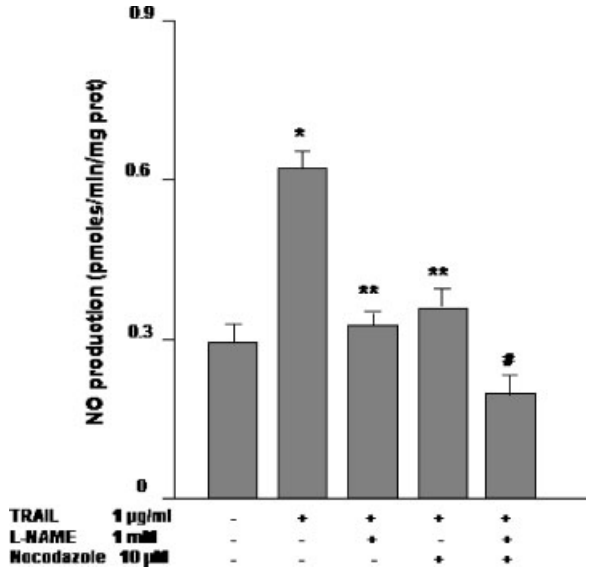

Fig. 6. TRAIL-increased total NOS activity. Total NOS activity was quantified in the cell lysates of HUVEC exposed for 10 min to different stimuli. Data, expressed as pmoles/min/mg proteins, are the mean values ± SD of three independent experiments ($^{*}P < 0.001$ vs. control, $^{**}P < 0.005$ vs. TRAIL, and $^{\#}P < 0.001$ vs. TRAIL).

DISCUSSION

Since a few years ago, the known biological activity of TRAIL was far limited to induce apoptosis in various cell lines [Wiley et al., 1995; Baker and Reddy, 1996]. In more recent years, although a role for TRAIL in physiologic conditions has not been clearly envisioned yet, a novel function of this cytokine is emerging in endothelial cell physiology regulation [Secchiero et al., 2003; Zauli et al., 2003; Di Pietro and Zauli, 2004]. It is known that PI3kinase (PI3k)/Akt pathway is essential for endothelial cell differentiation, migration, and NO production [Carmeliet, 2000]. To shed light into TRAIL-mediated physiologic effects, we previously demonstrated, in vascular endothelial cells, that TRAIL stimulates the PI3k-dependent phosphorylation of the serine/threonine kinase Akt [Secchiero et al., 2003] inducing, as a consequence, a time- and dose-dependent increase in NO production and a parallel significant increase in eNOS phosphorylation, NOS activity, and cGMP production [Zauli et al., 2003].

In this study, we have observed that TRAIL increases both extracellular and intracellular NO levels and causes a time-dependent NO spots migration, imaged by DAF-2DA fluorescence, from the cell plasma membrane to the inner part of the cell. Even though in our experiments the movement of NO spots was difficult to discern from cell movement due to shape changes induced by actin cytoskeleton remodeling [Sessa et al., 1995; Zauli et al., 2003], the possibility that TRAIL is itself able to induce eNOS cytoplasm translocation is supported by the significant increase in cytoplasm levels of eNOS (Fig. 3), which, moreover, appears co-localized with the Golgi apparatus at a higher extent than in the absence of stimulation (Fig. 4). It was interesting to note that TRAIL effects on eNOS trafficking were significantly inhibited in the presence of L-NAME (Fig. 3), indicating the NOS-derived NO dependency of these effects. According to the notion that the state of actin and microtubule polymerization can affect endothelial cell eNOS localization, activity and secondary NO production, it is conceivable that, in our cellular model, the TRAIL-induced NOS activity and NO release might in turn stimulate cytoskeleton reorganization. In fact, in our cellular model TRAIL induced the formation of trans-cytoplasm stress fibers without affecting the polymerization state of microtubule structures, which, instead, were clearly disrupted with Nocodazole treatment. This microtubule depolymerizing compound induced a significant decrease in NOS activity (Fig. 6), confirming the involvement of cytoskeleton components in the TRAIL-mediated increase in NOS activity. These observations, supported by the inhibitory effect of L-NAME both on TRAIL-stimulated NO release and intracellular targeting of eNOS, emphasize the importance of spatial localization of eNOS to lead to the consequent NO production. In fact, regulated location and trafficking of eNOS may be essential in regulating enzyme activity and maintaining the spatial and temporal organization of NO signaling in endothelial cells [Ortiz and Garvin, 2003]. Different mechanisms have been shown to control eNOS targeting from the Golgi apparatus to the plasma membrane, correct compartmentalization within the membrane, and internalization from the plasma membrane to the cytoplasm after activation. Previous works by some [Prabhakar et al., 1998; Ortiz and Garvin, 2003; Fulton et al., 2004] but not all laboratories [Haynes et al., 2000; McCabe et al., 2000; Govers et al., 2002] showed that

agonist-stimulated phosphorylation or depalmitoylation of eNOS may cause its translocation from membrane to cytosol. We can speculate that such a mechanism may occur also in our system since, upon TRAIL stimulation and in a time-dependent manner, a fraction of eNOS is no longer associated to membranes and becomes soluble in the cytoplasm or located at the Golgi complex, as demonstrated with double labeling immune fluorescence techniques. The functional role of Golgi complex-localized eNOS has been widely documented and, recently, Fulton et al. [2002] demonstrated the Ser1179 phosphorylation of Golgi complex-localized eNOS in response to VEGF, identifying "burst" of NO emanating from the peri-nuclear region of endothelial cells. Since in our previous study we demonstrated a TRAIL-increased eNOS phosphorylation [Zauli et al., 2003], we could hypothesize that a similar mechanism of action can occur in the TRAIL-mediated increase in NO production.

The mechanisms regulating the intracellular distribution of eNOS between the Golgi and plasma membrane pools and the physiological role underlying their distinct regulation remain to be established. However, it is conceivable that by influencing the relative proportion of eNOS in the Golgi complex versus the plasma membrane, the ability of an endothelial cell to respond to calcium- and Akt-dependent agonists can be modified. Thus, endothelial cell agonists that utilize primarily Akt-dependent mechanisms, such as VEGF, insulin, estrogen, and, very likely, TRAIL would preferentially activate Golgi-eNOS, while, conversely, calcium-dependent agonists such as thapsigargin and bradykinin would preferentially activate plasma membrane-eNOS [Fulton et al., 2004]. In this regard, it was previously demonstrated that an initially scattered Golgi structure, unlike a complete Golgi stack, should not be fully functional and decidedly enriched in trans-Golgi vesicles [Yang and Storrie, 1998] in which targeted eNOS displays a reduced basal and Akt-stimulated phosphorylation level [Fulton et al., 2004]. In this study, we used a more direct approach to induce an initial scattering of the Golgi apparatus with Nocodazole treatment (10 μM, 45 min) to then evaluate the extent of eNOS/Golgi co-localization which was significantly increased after treatment (Fig. 4). These results, supported by the parallel reduction of TRAIL-stimulated NOS activity induced by Nocodazole, strongly indicate that the blocking of eNOS in the trans-Golgi vesicles compromises the enzyme activity both in basal conditions and upon TRAIL stimulation (Fig. 6).

Several recent studies have shown that reorganization of the cytoskeleton, including actin filaments and microtubules, may affect eNOS activity, leading to the alteration of NO production [Ortiz and Garvin, 2003]. Actually, tubulin has been reported to be associated with Hsp90 and with Calmodulin [Redmond et al., 1989; Czar et al., 1996; Carraway et al., 1998] and Su et al. [2002] indicated that microtubule polymerization degree might modulate NO production by regulating the eNOS/Hsp90 interaction. More in detail, the authors have shown that pharmacological stabilization of microtubules results in an increase in NO production, whereas microtubule disruption decreases NO release, as demonstrated in cultured pulmonary artery endothelial cells under hypoxic conditions [Iwai et al., 1990]. In our cellular system, the absence of microtubule depolymerization upon TRAIL stimulation may favor the eNOS/Hsp90 association, leading to the consequent enhanced eNOS activity. Another connection between eNOS-mediated NO production and cytoskeleton was provided in a recent study published by Zharikov et al. [2001]. These investigators reported that pharmacological stabilization of actin polymerization increased arginine transport and NO production in porcine pulmonary artery endothelial cells, whereas pharmacological disruption of actin microfilaments decreased NO production. These data are consistent with our present and previous observations of the rapid formation of trans-cytoplasm stress fibers and the parallel significant increase in NO release upon TRAIL treatment.

In conclusion, in our cellular model TRAIL is able to activate eNOS and, consequently, to increase NO release through the regulation of enzyme localization among different subcellular compartments. Our data also demonstrate the involvement in this machinery of cytoskeleton components and Golgi apparatus and, altogether, add new important evidences to the potential physiological role of this pleiotropic molecule.

ACKNOWLEDGEMENTS

The authors thank Prof. Giorgio Fanò for critical review, Dr. Luciana Caravatta for

rTRAIL preparations, Dr. Natalia Di Pietro and Dr. Pamela Di Tomo for their assistance with tissue cultures.

REFERENCES

Ashkenazi A, Dixit VM. 1999. Apoptosis control by death and decoy receptors. Curr Opin Cell Biol 11:255–260.

Baker SJ, Reddy EP. 1996. Transducers of life and death: TNF receptor superfamily and associated proteins. Oncogene 12:1–9.

Busse R, Mulsch A. 1990. Calcium-dependent nitric oxide synthesis in endothelial cytosol is mediated by calmodulin. FEBS Lett 265:133–136.

Carmeliet P. 2000. Mechanisms of angiogenesis and arteriogenesis. Nat Med 6:389–395.

Carraway KL, Carraway CAC, Carraway KL III. 1998. Cell morphology and the cytoskeleton. In: Signaling and the cytoskeleton. New York: Springer-RG, Landes. pp 1–40.

Czar MJ, Welsh MJ, Pratt WB. 1996. Immunofluorescence localization of the 90-kDa heat-shock protein to cytoskeleton. Eur J Cell Biol 70:322–330.

Degli Esposti MA, Dougall WC, Smolak PJ, Waugh JY, Smith CA, Goodwin RG. 1997a. The novel receptor TRAIL-R4 induces NF-κB and protects against TRAIL-mediated apoptosis, yet retains an incomplete death domain. Immunity 7:813–820.

Degli Esposti MA, Smolak PJ, Walczak H, Waugh J, Huang CP, DuBose RF, Goodwin RG, Smith CA. 1997b. Cloning and characterization of TRAIL-R3, a novel member of the emerging TRAIL receptor family. J Exp Med 186:1165–1170.

Di Pietro R, Zauli G. 2004. Emerging non-apoptotic functions of tumor necrosis factor-related apoptosis-inducing ligand (TRAIL)/Apo2L. J Cell Physiol 201: 331–340.

Ehrhardt H, Fulda S, Schmid I, Hiscott J, Debatin K-M, Jeremias I. 2003. TRAIL induced survival and proliferation in cancer cells resistant towards TRAIL-induced apoptosis mediated by NF-κB. Oncogene 22:3842–3852.

Fulton D, Fontana J, Sowa G, Gratton JP, Lin M, Li KX, Michell B, Kemp BE, Rodman D, Sessa C. 2002. Localization of endothelial nitric-oxide synthase phosphorylated on serine 1179 and nitric oxide in Golgi and plasma membrane defines the existence of two pools of active enzyme. J Biol Chem 277:4277–4284.

Fulton D, Babbitt R, Zoellner S, Fontana J, Acevedo L, McCabe T, Iwakiri Y, Sessa WC. 2004. Targeting of endothelial nitric-oxide synthase to the cytoplasmic face of the Golgi complex or plasma membrane regulates Akt-versus calcium-dependent mechanisms for nitric oxide release. J Biol Chem 279:30349–30357.

Govers R, van der Sluijs P, van Donselaar E, Slot JW, Rabelink TJ. 2002. Endothelial nitric oxide synthase and its negative regulator Caveolin-1 localize to distinct perinuclear organelles. J Histochem Cytochem 50:779–788.

Haynes MP, Sinha D, Russel KS, Colline M, Fulton D, Morales-Ruiz M, Sessa WC, Bender JR. 2000. Membrane estrogen receptor engagement activates endothelial nitric oxide synthase via the PI3-kinase-Akt pathway in human endothelial cells. Circ Res 87:677–682.

Hobbs AJ, Higgs A, Moncada S. 1999. Inhibition of nitric oxide synthase as a potential therapeutic target. Annu Rev Pharmacol Toxicol 39:191–220.

Iwai K, Hori M, Kitabatake A, Kurihara H, Uchida K, Inoue M, Kamada T. 1990. Disruption of microtubules as an early sign of irreversible ischemic injury. Immunohistochemical study of in situ canine hearts. Circ Res 67:694–706.

McCabe TJ, Fulton D, Roman LJ, Sessa WC. 2000. Enhanced electron flux and reduced calmodulin dissociation may explain "calcium-independent" eNOS activation by phosphorylation. J Biol Chem 275:6123–6128.

Michel T. 1999. Targeting and translocation of endothelial nitric oxide synthase. Braz J Med Biol Res 32:1361–1366.

Michel T, Feron O. 1997. Nitric oxide synthases: Which, where, how, and why? J Clin Invest 100:2146–2152.

Misko TP, Schilling DS, Moore WM, Currie M. 1993. A fluorimetric assay for the measurement of nitrite in biological samples. Anal Biochem 214:11–16.

Ortiz PA, Garvin JL. 2003. Trafficking and activation of eNOS in epithelial cells. Acta Physiol Scand 179:107–114.

Pan G, O'Rourke K, Chinnaiyan AM, Gentz R, Ebner R, Ni J, Dixit VM. 1997. The receptor for the cytotoxic ligand TRAIL. Science 276:111–113.

Pandolfi A, Grilli A, Cilli C, Patruno A, Giaccari A, Di Silvestre S, De Lutiis MA, Pellegrini G, Capani F, Consoli A, Felaco M. 2003. Phenotype modulation in cultures of vascular smooth muscle cells from diabetic cats: Association with increased nitric oxide synthase expression and superoxidation generation. J Cell Physiol 196:378–385.

Prabhakar P, Thatte HS, Goetz RM, Cho MR, Golan DE, Michel T. 1998. Receptor-regulated translocation of endothelial nitric-oxide synthase. J Biol Chem 273:27383–27388.

Redmond T, Sanchez ER, Bresnick EH, Schlesinger MJ, Toft DO, Pratt WB, Welsh MJ. 1989. Immunofluorescence colocalization of the 90-kDa heat-shock protein and microtubules in interphase and mitotic mammalian cells. Eur J Cell Biol 50:66–75.

Secchiero P, Gonelli A, Celeghini C, Mirandola P, Guidotti L, Visani G, Capitani S, Zauli G. 2001. Activation of the nitric oxide synthase pathway represents a key component of tumor necrosis factor-related apoptosis-inducing ligand-mediated cytotoxicity on hematologic malignancies. Blood 98:2220–2228.

Secchiero P, Gonelli A, Carnevale E, Milani D, Pandolfi A, Zella D, Zauli G. 2003. TRAIL promotes the survival and proliferation of primary human vascular endothelial cells by activating the Akt and ERK pathways. Circulation 107:2250–2256.

Secchiero P, Melloni E, Heikinheimo M, Mannisto S, Di Pietro R, Iacone A, Zauli G. 2004. TRAIL regulates normal erythroid maturation through an ERK-dependent pathway. Blood 103:517–522.

Sessa WC, Garcia-Cardena G, Liu J, Keh A, Pollock JS, Bradley J, Thiru S, Braverman IM, Desai KM. 1995. The Golgi association of endothelial nitric oxide synthase is necessary for the efficient synthesis of nitric oxide. J Biol Chem 270:17641–17644.

Su Y, Zharikov SI, Block ER. 2002. Microtubule-active agents modify nitric oxide production in pulmonary artery endothelial cells. Am J Physiol Lung Cell Mol Physiol 282:L1183–L1189.

Walczak H, Degli Esposti MA, Johnson RS, Smolak PJ, Waugh JY, Boiani N, Timour MS, Gerhart MJ, Schooley KA, Smith CA, Goodwin RG, Rauch CT. 1997. TRAIL-R2: A novel apoptosis-mediating receptor for TRAIL. EMBO J 16:5386–5397.

Wiley SR, Schooley K, Smolak PJ, Din WS, Huang CP, Nicholl JK, Sutherland GR, Davis-Smith T, Rauch C, Smith CA, Goodwin RG. 1995. Identification and characterization of a new member of the TNF family that induces apoptosis. Immunity 3:673–682.

Yang W, Storrie B. 1998. Scattered Golgi elements during microtubule disruption are initially enriched in trans-Golgi proteins. Mol Biol Cell 9:191–207.

Zanella B, Calonghi N, Pagnotta E, Casotti L, Guarnirei C. 2002. Mitochondrial nitric oxide localization in H9c2 cells revealed by confocal microscopy. Biochem Biophys Res Commun 290:1010–1014.

Zauli G, Pandolfi A, Gonelli A, Di Pietro R, Guarnieri S, Ciabattoni G, Rana R, Vitale M, Secchiero P. 2003. Tumor necrosis factor-related apoptosis-inducing ligand (TRAIL) sequentially upregulates nitric oxide and prostanoid production in primary human endothelial cells. Circ Res 92:732–740.

Zhang XD, Nguyen T, Thomas WD, Sanders JE, Hersey P. 2000. Mechanisms of resistance of normal cells to TRAIL induced apoptosis vary between different cell types. FEBS Lett 482:193–199.

Zharikov SI, Sigova AA, Chen S, Bubb MR, Block ER. 2001. Cytosketetal regulation of the L-arginine/NO pathway in pulmonary artery endothelial cells. Am J Physiol Lung Cell Mol Physiol 280:L465–L473.